Wireless Communications Systems with Spatial Diversity: A Volumetric Approach

L. W. Hanlen and M. Fu
School of Electrical Engineering and Computer Science
The University of Newcastle
NSW 2308, Australia

Abstract— **This paper presents a new physical modelling approach for wireless systems with multiple antennas. The fundamental problem of modelling the communications channel if we are given an arbitrary spatial volume for transmitting, an arbitrary spatial volume for receiving, and a set of scattering bodies is studied. We show how to calculate the number of communication modes, both for direct (point-to-point) and for scattering environments. Our work explains the physical parameters which determine the channel model and its channel capacity.**

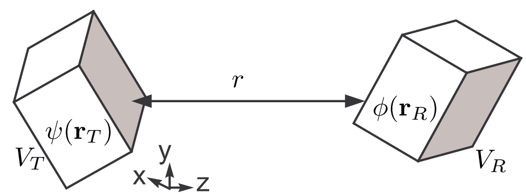

Fig. 1. Two volume arrangement for arbitrary volumes V_T and V_R

I. Introduction

Scattering has been shown to improve capacity for wireless communications. More specifically, the capacity of multi-antenna (MIMO) systems with dense scattering is shown to grow proportionally with the minimum of the number of transmitters and receivers [1], [2]. This is the well-known *linear growth* property of MIMO systems. However, the channel is assumed to be an identically distributed matrix [1], [2], and the high capacity is proved without verification on the validity of the channel model.

Recently some work has focused on the modelling of MIMO channels. In [3] correlated "pin hole" channels were introduced and other authors [4] have discussed the effects of antenna placement. This paper attempts to provide a more realistic physical model for multi-antenna systems. We ask: *how do we model the communications channel if we are given a spatial volume for transmitting, a spatial volume for receiving and a set of scattering bodies?* In addressing this question, we determine the number of communications modes (or degrees of freedom) for radio communications between two volumes. The case without scattering bodies has already been studied in [5] for optical communications.

We will first summarize the work of [5] in section II for the two body case. We then extend [5] in II-C to provide a numerical solution for channel modelling with arbitrary transmit and receive volumes. Section III provides a generalization of these results to include scattering bodies. Illustrative examples are used in section IV to compare direct transmission with transmission through a line-of-sight and non-line-of-sight scattering channel.

A part of this work was carried out while the authors visited Nanyang Technological University in Singapore. The authors would like to thank Nanyang Technological University for their support to this research.

II. Modelling for two volume communications

Consider wireless communications between two arbitrary volumes *in free space* as depicted in figure 1, where V_T is the transmitting body and V_R is the receiving body. The centres of the two bodies are separated by a distance r. It is assumed that the dimensions of the two bodies are small compared to the distance r. We choose the coordinates (x, y, z) such that the z-axis is along the distance r and the origin is the centre of the transmitting body. For simplicity, we consider monochromatic signals.

It was shown in [5] that if V_T and V_R are hyper-rectangles with sides parallel to the (x, y, z) axes and lengths $2\Delta x_T, 2\Delta y_T, 2\Delta z_T$ and $2\Delta x_R, 2\Delta y_R, 2\Delta z_R$, there is a simple expression for the transfer function from V_T to V_R. Indeed, the eigenfunctions for V_T (and those for V_R) can be expressed in terms of a focusing function and a set of prolate spheroidal functions. These eigenfunctions form a set of complete, orthonormal functions. Further, the corresponding singular values are roughly constant up to a critical number N_c beyond which they are negligible. N_c is the number of communications modes between V_T and V_R, given by

$$N_c = \frac{V_R V_T}{r^2 \lambda^2 (2\Delta z_T)(2\Delta z_R)} \quad (1)$$

where (with slight abuse of notation) V_T and V_R are the volumes of the two bodies and λ is the wavelength of the transmit signal. Consequently, the transfer function between V_T and V_R is given by a diagonal matrix of a finite dimension, with the diagonal elements being the non-negligible singular values.

A. Transfer Function

Let $\psi(\mathbf{r}_T)$ represent the source function at a point $\mathbf{r}_T \in V_T$ and $\phi(\mathbf{r}_R)$ be the received electromagnetic field at a point $\mathbf{r}_R \in V_R$. Then $\phi(\mathbf{r}_R)$ is given by

$$\phi(\mathbf{r}_R) = \int_{V_T} G(\mathbf{r}_R, \mathbf{r}_T)\psi(\mathbf{r}_T)d^3\mathbf{r}_T \tag{2}$$

where $G(\mathbf{r}_R, \mathbf{r}_T)$ is the (retarded) Green's function defined by

$$G(\mathbf{r}_R, \mathbf{r}_T) = \frac{\exp(-\iota k|\mathbf{r}_R - \mathbf{r}_T|)}{4\pi|\mathbf{r}_R - \mathbf{r}_T|} \tag{3}$$

where $\iota = \sqrt{-1}$, $k = 2\pi/\lambda$, and λ is the signal wavelength.

In order to calculate connection strengths between $\psi(\mathbf{r}_T)$ and $\phi(\mathbf{r}_R)$ we require a set of basis functions. Define $\{\alpha_{Ti}(\mathbf{r}_T), i = 1, \cdots, N_T\}$ as a finite set of orthonormal functions in V_T. Likewise, define $\{\alpha_{Ri}(\mathbf{r}_R), i = 1, \cdots, N_R\}$ to be a finite orthonormal set of functions in V_R.

Given a transmitting function $\alpha_{Ti}(\mathbf{r}_T)$, the received signal is given by application of (2):

$$\phi_i(\mathbf{r}_R) = \int_{V_T} G(\mathbf{r}_R, \mathbf{r}_T)\alpha_{Ti}(\mathbf{r}_T)d^3\mathbf{r}_T \tag{4}$$

We may then decompose $\phi_i(\mathbf{r}_R)$ into components of $\alpha_{Rj}(\mathbf{r}_R)$. Define the projection of $\phi_i(\mathbf{r}_R)$ on $\alpha_{Rj}(\mathbf{r}_R)$ as:

$$\begin{aligned}\gamma_{ji} &= \int_{V_R} \alpha^*_{Rj}(\mathbf{r}_R)\phi_i(\mathbf{r}_R)d^3\mathbf{r}_R \\ &= \int_{V_R}\int_{V_T} \alpha^*_{Rj}(\mathbf{r}_R)G(\mathbf{r}_R, \mathbf{r}_T)\alpha_{Ti}(\mathbf{r}_T)d^3\mathbf{r}_T d^3\mathbf{r}_R \end{aligned} \tag{5}$$

Then, we have

$$\phi_i(\mathbf{r}_R) = \sum_{j=1}^{N_R} \gamma_{ji}\alpha_{Rj}(\mathbf{r}_R) + \delta\phi_i(\mathbf{r}_R) \tag{6}$$

where $\delta\phi_i(\mathbf{r}_R)$ is a residual term orthogonal to all $\alpha_{Rj}(\mathbf{r}_R)$.

Take any transmitting signal as

$$\psi(\mathbf{r}_T) = \sum_{i=1}^{N_T} a_i\alpha_{Ti}(\mathbf{r}_T) \tag{7}$$

The received signal will be

$$\begin{aligned}\phi(\mathbf{r}_R) &= \sum_{i=1}^{N_T} a_i \left(\sum_{j=1}^{N_R} \gamma_{ji}\alpha_{Rj}(r_R)\right) + \delta\phi(\mathbf{r}_R) \\ &= \sum_{j=1}^{N_R} b_j\alpha_{Rj}(\mathbf{r}_R) + \delta\phi(\mathbf{r}_R)\end{aligned} \tag{8}$$

where $\delta\phi(\mathbf{r}_R)$ is a residual signal orthogonal to all $\alpha_{Rj}(\mathbf{r}_R)$. Let a_i and b_j be the coefficients of the projections of $\psi(\mathbf{r}_T)$ onto $\alpha_{Ti}(\mathbf{r}_T)$ and $\phi(\mathbf{r}_R)$ onto $\alpha_{Rj}(\mathbf{r}_R)$, respectively. Then, we have

$$b_j = \sum_{i=1}^{N_T} a_i\gamma_{ji} \qquad \text{or} \qquad b = \Gamma a \tag{9}$$

If $N_T = N_R \to \infty$ and the sets $\{\alpha_{Ti}(\mathbf{r}_T)\}$ and $\{\alpha_{Rj}(\mathbf{r}_R)\}$ are complete, then any transmitting signal can be expressed as in (8) without the residual term $\delta\phi(\mathbf{r}_R)$. In this case, (9) represents the true transfer function of the communications system.

B. Eigenfunctions

If r is large compared to V_T and V_R, we may approximate $|\mathbf{r}_R - \mathbf{r}_T|$ [5] by:

$$|\mathbf{r}_R - \mathbf{r}_T| \approx r + z_R - z_T + \frac{(x_R - x_T)^2 + (y_R - y_T)^2}{2r} \tag{10}$$

This leads to a separation of $\alpha_i(\mathbf{r}_T)$:

$$\alpha_{Ti}(\mathbf{r}_T) = F_T(\mathbf{r}_T)\beta_{Ti}(x_T, y_T) \tag{11}$$

where $\beta_{Ti}(x_T, y_T)$ are new functions and $F_T(\cdot)$ is the so-called *focusing function* defined by

$$F_T(\mathbf{r}_T) = \exp\left(-\iota k(z_T - \frac{x_T^2}{2r} - \frac{y_T^2}{2r})\right) \tag{12}$$

A similar separation may be performed for $\alpha_{Ri}(\mathbf{r}_R)$.

C. Numerical Solutions

We first consider the case where both V_T and V_R are hyper-rectangles with faces parallel to the x, y, z axes. Suppose the dimensions of V_T are given by $2\Delta x_T$, $2\Delta y_T$ and $2\Delta z_T$, and similarly for V_R. This case is analysed in [5] and the solution is given as follows:

$$\beta_{T(m,n)}(x_T, y_T) = S_{0m}(c_x, \hat{x}_T)S_{0n}(c_y, \hat{y}_T) \tag{13}$$

for $m, n = 0, 1, \cdots$, where

$$c_x = \frac{k\Delta x_T \Delta x_R}{r}, \qquad \hat{x}_T = \frac{x_T}{\Delta x_T} \tag{14}$$

and similarly for c_y and $\hat{y}_T$. and $S_{0m}(c, \xi)$ is the so-called $(0, m)$th angular prolate spheroidal function given by

$$v_m S_{0m}(c_x, \xi) = \int_{-1}^{1} \frac{\sin(c(\xi - \xi^{'}))}{\pi(\xi - \xi^{'})} S_{0m}(c, \xi^{'})d\xi^{'} \tag{15}$$

where v_m are the singular values with $1 > |v_1| > |v_2| > \cdots > 0$. Only a finite number of v_i have non-negligible values. The functions $S_{0m}(c, \xi)$ are well studied. Computational methods are available in [6] and [7]. The functions $\beta_{R(m,n)}(\mathbf{r}_R)$ can be expressed in a similar fashion to (13).

For the general case where V_T and V_R take arbitrary shapes, the basis functions $\beta_{Ti}(x_T, y_T)$ and $\beta_{Ri}(x_R, y_R)$ are not separable. Although we could return to the original integral equations [5], such an approach is computationally expensive. The following alternate approach is proposed:

1) Project V_T onto the (x, y) plane to obtain a surface S_T. Then take $\bar{S}_T$ to be the smallest bounding rectangle containing S_T, which is parallel to the (x, y) axes. Let $2\Delta x_T$ and $2\Delta y_T$ be the lengths of $\bar{S}_T$ in x and y directions, respectively. Repeat for V_R and obtain S_R, $\bar{S}_R$, $2\Delta x_R$ and $2\Delta y_R$.
2) Compute $\bar{\beta}_{Ti}(x_T, y_T)$ as in (13) and similarly for $\bar{\beta}_{Ri}(x_R, y_R)$ using $\bar{S}_T$ and $\bar{S}_R$.
3) By definition, the set $\bar{\beta}_T(x_T, y_T) = \{\bar{\beta}_{Ti}(x_T, y_T)\}$ is complete in $\bar{S}_T$. It is also complete in S_T (but not necessarily orthonormal). To see this, consider a function $f(x_T, y_T)$ which is zero for all (x_T, y_T) outside of S_T. $f(x_T, y_T)$ may be expressed as a linear combination of $\bar{\beta}_{Ti}(x_T, y_T)$ over $\bar{S}_T$ since $\{\bar{\beta}_{Ti}(x_T, y_T)\}$ is a complete set in $\bar{S}_T$. The same combination still holds over S_T because $S_T \subset \bar{S}_T$. A similar claim holds for $\beta_R(x_R, y_R)$.
4) Transform the set $\{\bar{\beta}_{Ti}(x_T, x_y)\}$ to another set $\{\tilde{\beta}_{Ti}(x_T, y_T)\}$ which is complete and orthonormal in S_T. This may be done, using the Gram-Schmidt process as follows:
$$\tilde{\beta}_{T1}(x_T, y_T) = \frac{\bar{\beta}_{T1}(x_T, y_T)}{\|\bar{\beta}_{T1}(x_T, y_T)\|_{S_T}} \tag{16}$$
where
$$\|\bar{\beta}_{T1}(x_T, y_T)\|^2_{S_T} = \int_{S_T} \bar{\beta}^*_{T1}(x_T, y_T)\bar{\beta}_{T1}(x_T, y_T)\, dx_T dy_T \tag{17}$$
Then, for $i = 2, 3, \cdots, N$ define:
$$\check{\beta}_{Ti} \Leftarrow \bar{\beta}_{Ti} - \sum_{j=1}^{i-1} \bar{\beta}_{Tj} \cdot \langle \bar{\beta}_{Ti}, \tilde{\beta}_{Tj} \rangle \tag{18}$$
If the remaining function $\check{\beta}_{Ti}$ is zero, ignore it; otherwise, normalise it (in S_T) and we obtain $\tilde{\beta}_{Ti}(x_T, y_T)$. Transform the set $\{\bar{\beta}_{Ri}(x_R, y_R)\}$ to $\{\tilde{\beta}_{Ri}(x_R, y_R)\}$ in a similar way.
5) Define
$$\tilde{\alpha}_{Ti}(\mathbf{r}_T) = F_T(\mathbf{r}_T)\tilde{\beta}_{Ti}(x_T, y_T) \tag{19}$$
and similarly for $\tilde{\alpha}_{Rj}(\mathbf{r}_R)$.
6) The transfer coefficient γ_{ji} from $\tilde{\psi}_i(\mathbf{r}_T)$ in V_T to $\tilde{\phi}_j(\mathbf{r}_R)$ in V_R may now be computed. The approximation (10) gives
$$G(\mathbf{r}_R, \mathbf{r}_T) \approx \frac{\exp(-\iota kr)}{4\pi r} F_T(\mathbf{r}_T)F_R(\mathbf{r}_T) \cdot \exp\left(\frac{\iota k}{r}(x_R x_T + y_R y_T)\right)$$
It follows that
$$\gamma_{ji} = \frac{\exp(-\iota kr)}{4\pi r} \cdot \iint_{V_R V_T} \tilde{\beta}^*_{Rj}(x_R, y_R) \cdot \exp\left(\frac{\iota k}{r}(x_R x_T + y_R y_T)\right) \tilde{\beta}_{Ti}(x_T, y_T) d^3\mathbf{r}_T d^3\mathbf{r}_R \tag{20}$$
Since the integrand is independent of z_T and z_R, we simplify (20) to:
$$\gamma_{ji} = \frac{\exp(-\iota kr)}{4\pi r} \int_{S_R} 2\Delta z_R(x_R, y_R)\tilde{\beta}^*_{Rj}(x_R, y_R) \cdot f(x_R, y_R) dx_R dy_R \tag{21}$$
$$f(x_R, y_R) = \int_{S_T} 2\Delta z_T(x_T, y_T) \cdot \exp\left(\frac{\iota k}{r}(x_R x_T + y_R y_T)\right) \tilde{\beta}_{Ti}(x_T, y_T) dx_T dy_T \tag{22}$$
where $2\Delta z_T(x_T, y_T)$ is the thickness of V_T in the z direction at (x_T, y_T), and $2\Delta z_R(x_R, y_R)$ is similarly defined.

D. Simplification of Transfer Function

In practice, we only need to compute a finite number of terms of γ_{ji}, i.e. we obtain a truncated Γ. This raises the question of whether the numerical solution is sufficiently accurate. The accuracy of the numerical solution may be estimated via the well-known *sum rule* [5]. If $\{\tilde{\psi}_i(\mathbf{r}_T)\}$ and $\{\tilde{\phi}_j(\mathbf{r}_R)\}$ are complete orthonormal basis functions for V_T and V_R, respectively, then under the assumption that the dimensions of V_T and V_R are sufficiently small, we have
$$\sum_{i,j} |\gamma_{ji}|^2 \approx \frac{V_T V_R}{(4\pi r)^2} \tag{23}$$
If Γ is truncated, the left-hand side of (23) always reduces. Hence, if (23) holds sufficiently close, we know that the numerical solution is sufficiently accurate. If the sum of $|\gamma_{ji}|^2$ is too small, then we need to compute a larger Γ, that is, calculate a larger number of basis functions. As a rule of thumb, we may start the size of the truncated Γ to be $\bar{N}_c \times \bar{N}_c$, where $\bar{N}_c$ is the number of communicate modes for $(\bar{S}_T, \bar{S}_R)$.

In general, $\tilde{\alpha}_{Ti}(\mathbf{r}_T)$ and $\tilde{\alpha}_{Rj}(\mathbf{r}_R)$ are not the eigenfunctions of Γ. As such, we may need to calculate more basis functions than there are communication modes, in order to satisfy the sum-rule. In order to obtain a minimal representation of Γ, a singular value decomposition of Γ is performed
$$\Gamma = U^* \Lambda V \tag{24}$$
where U and V are unitary matrices and Λ is a diagonal matrix containing the singular values of Γ in a descending order.

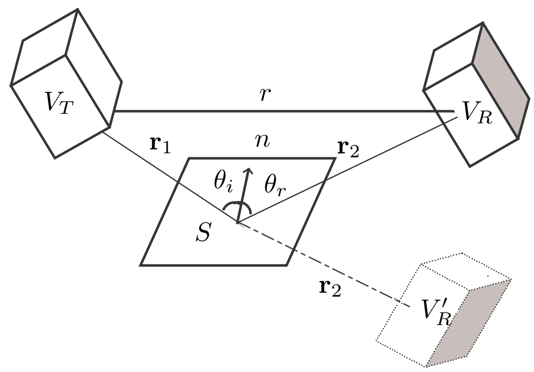

Fig. 2. Two volume arrangement, V_T and V_R with reflected volume V_R'

III. Modelling with Scattering Bodies

Consider the following thought experiment. We place an infinite plane P_z placed at a point z between two communicating bodies V_T and V_R (such as in figure 1) with an arbitrary normal direction $\mathbf{n}$. The plane absorbs all incident energy except for a hole $S(z, \mathbf{n})$ in the middle. We ask *how large must this hole be so that communications between the two volumes is not changed?*

If λ is sufficiently small, then $S(z, \mathbf{n})$ is the minimum area containing all the intersection points of P_z and $\ell(\mathbf{r}_T, \mathbf{r}_R)$, where $\ell(\mathbf{r}_T, \mathbf{r}_R)$ is the line linking $\mathbf{r}_T \in V_T$ and $\mathbf{r}_R \in V_R$. If λ is not sufficiently small, $S(z, \mathbf{n})$ needs to be enlarged by several wavelengths in each direction so that diffractions on the edges will be negligible.

We will call $S(z, \mathbf{n})$ the *viewing area* (with respect to P_z).

A. Single Scatterer

Consider now, a single scatterer S between two volumes, as depicted in figure 2. We assume that S is a purely reflective plane, i.e., there is no penetration of electric field. The reflection angle θ_r is the same as the incident angle θ_i, but the reflective electric field involves some possible loss which is represented by:

$$\eta(\theta_i) = \exp\left\{\left(\frac{\pi}{\lambda}\sigma_h \cos\theta_i\right)^2\right\} J_0\left\{8\left(\frac{\pi}{\lambda}\sigma_h \cos\theta_i\right)^2\right\} \qquad (25)$$

where σ_h is the standard deviation of the surface height, and $J_0(\cdot)$ is the modified Bessel function of order zero [8]. For a perfectly flat plane, $\sigma_h = 0$ and $\eta(\theta_i) = 1$.

The normal angle $\mathbf{n}$ of the scatterer needs to be such that the reflected signals are directed at V_R so that signal transmission from V_T to V_R is possible. To determine the reflected electrical field at V_R, we mirror-image V_R with respect to the scatterer (as shown by V_R' in figure 2). The scatterer may be viewed as the "hole" through which communications between V_T and mirror-imaged V_R takes place. The area of S must be larger than the corresponding viewing area between V_T and V_R' in order for V_T to fully communicate with V_R. We will call this viewing area a *reflective viewing area*. Once this condition holds, the transfer function between V_T and V_R may be computed using the result of section II-C, with the following modifications:

(i) the propagation distance increases to $r_s = r_1 + r_2$;
(ii) V_R' (not V_R) is used for computing the singular values and eigenfunctions of the channel model;
(iii) the computed eigenfunctions for V_R' must be mirror-imaged back so they become eigenfunctions for V_R.

Note that the same result can be obtained by mirror-imaging V_T due to the symmetry between transmission and reception.

B. Multiple Scatterers

Each scatterer $S_{(k)}, k = 1, \cdots, K$ provides a communications path. The transfer function $\Gamma^{(k)}$ for each path can be calculated using the method above. We may not simply sum the individual $\Gamma^{(k)}$, however, to obtain the overall transfer function Γ as each $\Gamma^{(k)}$ uses different eigenfunctions.

To obtain the correct Γ, we denote by $\{\alpha_{Ti}^{(k)}(\mathbf{r}_T)\}$ and $\{\alpha_{Ri}^{(k)}(\mathbf{r}_R)\}$ the two sets of eigenfunctions corresponding to $\Gamma^{(k)}$ and let the dimension of $\Gamma^{(k)}$ be $N_c^{(k)} \times N_c^{(k)}$. Then we have the following mapping:

$$\{\alpha_{Ti}^{(k)}(\mathbf{r}_T)\} \overset{\Gamma^{(k)}}{\longmapsto} \{\alpha_{Ri}^{(k)}(\mathbf{r}_R)\} \qquad (26)$$

Let $\{\Psi_i(\mathbf{r}_T)\}$ and $\{\Phi_i(\mathbf{r}_R)\}$ be any sets of complete, orthonormal basis functions for V_T and V_R, respectively. We can project each $\alpha_{Ti}^{(k)}(\mathbf{r}_T)$ onto $\Psi_j(\mathbf{r}_T), j = 1, 2 \cdots$ to obtain the following:

$$\alpha_{Ti}^{(k)}(\mathbf{r}_T) = \sum_{j=1}^{\infty} \gamma_{ij}^{(k)} \Psi_j(\mathbf{r}_T) \qquad (27)$$

where $\gamma_{ij}^{(k)}$ are projection coefficients. In vector form:

$$\alpha_T^{(k)}(\mathbf{r}_T) = \Gamma_\psi^{(k)} \Psi(\mathbf{r}_T) \qquad (28)$$

A similar projection can be obtained on the receiver side:

$$\Phi(\mathbf{r}_R) = \Gamma_\phi^{(k)} \alpha_R^{(k)}(\mathbf{r}_R) + \delta\alpha_R^{(k)}(\mathbf{r}_R) \qquad (29)$$

where $\delta\alpha_R^{(k)}(\mathbf{r}_R)$ is the residual term orthogonal to all $\alpha_{Rj}^{(k)}(\mathbf{r}_R)$. With the projections of (28) and (29) the overall transfer function is given by

$$\Gamma = \sum_{k=1}^{K} \Gamma_\phi^{(k)} \Gamma^{(k)} \Gamma_\psi^{(k)} \qquad (30)$$

As there is no sum-rule in this case, large sizes for $\Gamma_\phi^{(k)}$ and $\Gamma_\psi^{(k)}$ may be required to ensure numerical accuracy.

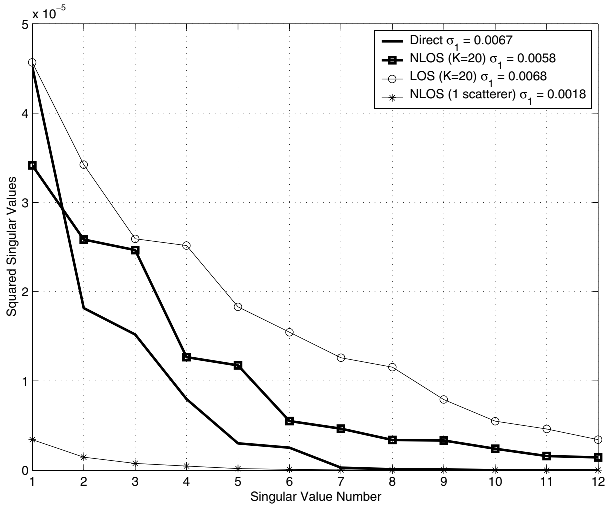

Fig. 3. Squared singular values of transfer

The growth in channel capacity can be explained intuitively as follows. Assume that the scatterers are local to either V_T or V_R. The strengths of different paths are similar, but their eigenfunctions may be very different: For different scatterers the effective propagation distances are roughly the same. However, different mirror-imaged bodies are obtained and used for computing the eigenfunctions. Since mirror-imaging does not diminish the volume, the connection strengths are not decreased.

Each new scatterer provides a new pair of basis function sets. The components of the sets which are orthogonal to existing eigenfunctions will allow new modes of communications. The remaining components will contribute to the gain. The so-called "rich" scattering is observed where scatterers introduce new communication modes.

IV. Simulation

We compared a direct (non-scattering) transmission with various scattering environments. We considered a 3GHz, transmission frequency, giving $\lambda = 0.1m$. The volumes V_T and V_R were hyper-rectangles. V_T had side-lengths of $15\lambda \times 9\lambda \times 9\lambda$ and V_R had side-lengths of $18\lambda \times 9\lambda \times 9\lambda$. The volumes were separated by $r = 10m$. For this arrangement the number of communications modes for direct transmission (1) is $N_c \approx 2.6$. We have used [9] for the numerical computation of (13). Scatterers were modelled as planes with a gain $\eta = 1$. Each scatterer was placed in a random location, between V_T and V_R, with a random orientation.

Figure 3 shows the squared singular values for the different cases. Direct transmission is shown solid. The singular values $\hat{\sigma}_k$ can be seen to drop sharply beyond $k = 3$. Using the same arrangement, we introduced scattering, in both a non-line of sight and line-of-sight case.

The non-line-of-sight (NLOS) transmission is shown by the solid line, with squares. In this situation, transmission was possible only via the reflective scatterers. We used $K = 20$ scatterers. As can be seen, scattering has provided approximately double the number of equal-strength communications modes than were available in the direct transmission case.

This case may be compared with the single scatterer channel, shown by the asterisk line where a scatterer was placed randomly between V_T and V_R. As can be seen the channel gain in this case is significantly reduced.

The line-of-sight case (LOS) is shown by the circled line. Here communication occurred via both scattering ($K = 20$) and direct transmission. Comparing with NLOS, we see a significant improvement in the number of effective communication modes and their strengths as expected.

V. Conclusions

Connection strengths of continuous transmission modes between volumes provide an upper bound on MIMO channel capacity. We have presented a modelling approach for computing the connection strengths between two arbitrary volumes, both for direct (point-to-point) and for scattering environments. We have shown that scatterers may improve wireless communications by providing new communication modes and thus increasing N_c. This is the well known "rich scattering" case. Scatterers may also increase the gain of already available modes such as when LOS components are present. The continuous modelling approach frees us from unrealistic results of considering many antennas in small volumes and provides a mechanism for considering free space as a continuous, not discrete, medium.

References

[1] G. Foschini and M. Gans, "On limits of wireless communications in a fading environment when using multiple antennas," *Wireless Personal Communications*, vol. 6, pp. 311–335, 1998.

[2] I. Telatar, "Capacity of multi-antenna gaussian channels," *European Transactions on Telecommunications*, vol. 10, no. 6, pp. 585–595, Nov. 1999.

[3] D. Gesbert, H. Bölcskei, D. Gore, and A. Paulraj, "MIMO wireless channels: Capacity and performance prediction," in *IEEE Global Telecommunications Conference, Globecom'00*, vol. 2, 2000, pp. 1083–1088.

[4] N. Chiurtu, B. Rimoldi, and E. Telatar, "Dense multiple antenna systems," in *IEEE Information Theory Workshop*, Cairns, Australia, Sept. 2–7 2001, pp. 108–109.

[5] D. Miller, "Communicating with waves between volumes: evaluating orthogonal spatial channels and limits on coupling strengths," *Applied Optics*, vol. 39, no. 11, pp. 1681–1699, Apr. 2000.

[6] C. Flammer, *Spheroidal Wave Functions*. Stanford U. Press, Stanford, Calif., 1957.

[7] B. Frieden, "Evaluation, design and extrapolation methods for optical signals, based on use of the prolate functions," *Progress in Optics IX*, pp. 311–407, 1971.

[8] M. Martone, *MultiAntenna Digital Radio Transmission*, ser. mobile comunications series. Artech House, 2001.

[9] W. Thompson, *Atlas for Computing Mathematical Functions*. John Wiley & Sons, 1997.